Available online at www.sciencedirect.com

ScienceDirect

Nuclear Physics B 952 (2020) 114921

NUCLEAR PHYSICS B

www.elsevier.com/locate/nuclphysb

# Constraints on the Higgs boson anomalous FCNC interactions with light quarks

M. Ilyushin [a], P. Mandrik [a,b,*], S. Slabospitskii [a,b]

[a] *NRC "Kurchatov Institute" - IHEP, Protvino, Moscow Region, Russia*
[b] *Moscow Institute of Physics and Technology, Dolgoprudny, Moscow Region, Russia*

Received 13 May 2019; received in revised form 27 November 2019; accepted 6 January 2020
Available online 9 January 2020
Editor: Hong-Jian He

**Abstract**

We consider the Higgs boson anomalous FCNC interactions with $u$, $c$, $d$, $s$ and $b$ quarks using the effective field theory framework. Constraints on anomalous couplings are derived from experimental results on Higgs boson production with subsequent decay into $b\bar{b}$ pair at LHC with $\sqrt{s} = 13$ TeV. Upper limits on the branching fractions of $H \to b\bar{s}$ and $H \to b\bar{d}$ are set by performing a realistic detector simulation and accurately reproducing analysis selections of the CMS Higgs boson measurement in the four-lepton final state at $\sqrt{s} = 13$ TeV. The searches are projected into operation conditions of HL-LHC. Sensitivity at FCC-hh to anomalous FCNC interactions is studied based on Higgs boson production with $H \to \gamma\gamma$ decay channel. It is shown that at FCC-hh machine one can expect to set the upper limits of the order of $10^{-2}$ at 95% CL for $\mathcal{B}(H \to b\bar{s})$ and $\mathcal{B}(H \to b\bar{d})$.


## 1. Introduction

The discovery of Higgs boson by the Large Hadron Collider (LHC) [1,2] experiments has opened up new area of direct searches for physics Beyond Standard Model (BSM). One of the possible anomalous interaction is the Higgs-mediated flavor-changing neutral currents (FCNC). These processes are forbidden in Standard Model (SM) at tree level and are strongly suppressed in loop corrections by the Glashow-Iliopoulos-Maiani mechanism [3].

* Corresponding author.
*E-mail address:* petr.mandrik@ihep.ru (P. Mandrik).

https://doi.org/10.1016/j.nuclphysb.2020.114921

Table 1
The current experimental upper limits on FCNC decays of top-quark at 95% CL.

| Detector | $\mathcal{B}(t \to uH)$ | $\mathcal{B}(t \to cH)$ | Ref. |
|---|---|---|---|
| ATLAS, 13 TeV, 36.1 fb$^{-1}$ | $1.2 \times 10^{-3}$ | $1.1 \times 10^{-3}$ | [7] |
| CMS, 13 TeV, 35.9 fb$^{-1}$ | $4.7 \times 10^{-3}$ | $4.7 \times 10^{-3}$ | [9] |

Table 2
The upper limits on FCNC decays of Higgs boson to the light quarks at 95% CL from experiments with mesons (see [10] for details).

| Observable | Constraint |
|---|---|
| $D^0$ oscillations | $\mathcal{B}(H \to u\bar{c}) \lesssim 2 \times 10^{-5}$ |
| $B_d^0$ oscillations | $\mathcal{B}(H \to d\bar{b}) \lesssim 8 \times 10^{-5}$ |
| $K^0$ oscillations | $\mathcal{B}(H \to d\bar{s}) \lesssim 2 \times 10^{-6}$ |
| $B_s^0$ oscillations | $\mathcal{B}(H \to s\bar{b}) \lesssim 7 \times 10^{-3}$ |

The Higgs mediated FCNC in top-quark sector is actively investigated at LHC [4–9]. The main analyses strategy is to search for $t\bar{t}$ production with one top quark decay through a FCNC channel and other follow the dominant SM decay $t \to bW$. In [9] production of single top quark through a FCNC in association with the Higgs boson is considered in additional. The results of the searches are summarized in Table 1.

The FCNC couplings of the Higgs to the rest SM quarks can affect various low-energy precision measurements. The strongest indirect bounds on FCNC quark-quark-Higgs couplings came from measurement of $B_{d,s} - \bar{B}_{d,s}$, $K^0 - \bar{K}^0$ and $D^0 - \bar{D}^0$ oscillations [10]. The corresponding constraints on FCNC couplings translated into upper limits on branching fractions of the FCNC decays of Higgs boson to $u, d, s, c, b$ quarks are summarized in the Table 2. Due to huge QCD background the experiments at LHC are less sensitive to searching for FCNC decays of the Higgs boson. On the other hand the direct probes of such processes could complement the indirect limits. In addition in possible BSM scenarios the branching ratio of $H \to qq'$ can be enhanced with keeping other low-energy flavor observables approximately at their SM values [11,12]. Therefor, the searches for FCNC Higgs boson interactions are very important and could be considered as a complementary probe of new physics.

At the moment there is no any experimental evidence of the FCNC process. Future research and increase of the experimental sensitivity are related to the proposed energy-frontier colliders [13–16] such as High Luminosity LHC (HL-LHC) [17] and Future Circular Collider (FCC-hh) project, defined by the target of 100 TeV proton-proton collisions with a total integrated luminosity of 30 ab$^{-1}$ [18,19].

In this article we invested the contribution of FCNC interactions to the single Higgs boson production (Fig. 1, left) and Higgs boson production in association with a light quark (Fig. 1, center and right). The limits on Higgs boson FCNC interactions based on recent LHC data are obtained and the searches are projected into operation conditions of HL-LHC [17] and FCC-hh projects.

## 2. The constraints from the current Higgs production cross-sections

The flavor-violating couplings may arise from different sources [20]. In this article we use the effective field theory approach (EFT) [21–23] for describing the effects of BSM physics in Higgs

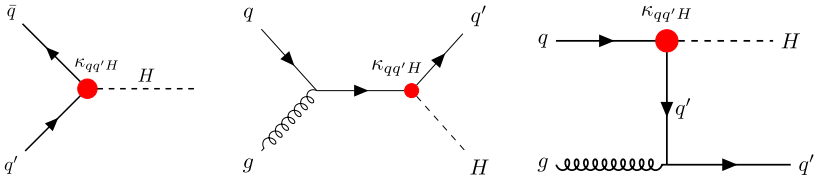


Fig. 1. Example of diagrams for Higgs boson production (left) and Higgs boson associated production with quark (center and right) mediated by FCNC couplings.

interactions. The effective Lagrangian (up to dimension-six gauge-invariant effective operators) has the form as follows [24,25]:

$$\mathcal{L}_{BSM} = -\frac{1}{\sqrt{2}}\bar{q}(\kappa^L_{qq'H}P_L + \kappa^R_{qq'H}P_R)q'H \tag{1}$$

where $P_{L,R} = \frac{1}{2}(1 \pm \gamma^5)$, $q, q' \in (u, c, t)$ or $q, q' \in (d, s, b)$. The couplings $\kappa^L_{qq'H}$ and $\kappa^R_{qq'H}$ are complex in general.

Note, that in our analysis these couplings are appeared in the combination

$$|\kappa^L_{qq'}|^2 + |\kappa^R_{qq'}|^2 = (\mathrm{Re}\,\kappa^L_{qq'})^2 + (\mathrm{Im}\,\kappa^L_{qq'})^2 + (\mathrm{Re}\,\kappa^R_{qq'})^2 + (\mathrm{Im}\,\kappa^R_{qq'})^2$$

Thus, in what follows we set

$$\left.\begin{array}{l} \kappa \equiv |\kappa^L_{qq'}| = |\kappa^R_{qq'}| \\ \lambda \equiv |\mathrm{Re}\,\kappa^L_{qq'}| = |\mathrm{Im}\,\kappa^L_{qq'}| = |\mathrm{Re}\,\kappa^R_{qq'}| = |\mathrm{Im}\,\kappa^R_{qq'}| \\ \rightarrow \kappa = \sqrt{2}\lambda \end{array}\right\} \tag{2}$$

The Higgs decays width resulted from (1) equals:

$$\Gamma(H \rightarrow q\bar{q}') = \frac{3(|\kappa^L_{qq'}|^2 + |\kappa^R_{qq'}|^2)M_H}{32\pi} = \frac{6|\lambda_{qq'}|^2 M_H}{16\pi} = |\lambda_{qq'}|^2 \times 14.92\ \text{GeV} \tag{3}$$

The very rough estimate of the coupling $\lambda_{qq'}$ (actually in order of magnitude) could be obtained from the measurement of the Higgs boson total decay width. The CMS collaboration presents the constraint of on the Higgs boson total width [26]:

$$\Gamma_H = 3.2^{+2.8}_{-2.2} \quad \text{MeV} \ @\ 68\%\ CL \tag{4}$$

$$\Gamma_H = [0.08 \div 9.16]\ \text{MeV} \ @\ 95\%\ CL \tag{5}$$

We use the value of 9.16 MeV from (5) as an upper limit on $\Gamma_H$. Then one gets:

$$\Gamma^{SM}_H + 2\Gamma(H \rightarrow q\bar{q}') \leq 9.16\,\text{MeV},\ \ \Gamma^{SM}_H = 4.1\ \text{MeV}$$
$$\Rightarrow |\lambda_{qq'}| \leq 0.013 \tag{6}$$

The more realistic estimates of the coupling $\lambda_{qq'}$ could be obtained from the Higgs production in the $pp$-collisions at LHC [27,28]:

$$pp \rightarrow H\,X,\ \ pp \rightarrow H\,W/Z\,X,\quad H \rightarrow b\bar{b} \tag{7}$$

We use the experimental results from ATLAS and CMS collaborations:

$$\mu_b = \frac{\sigma^{exp}(pp \rightarrow H\,X, H \rightarrow b\bar{b})}{\sigma^{theor}(pp \rightarrow H\,X, H \rightarrow b\bar{b})} \tag{8}$$

| | $pp \to H\,W/Z\,X$ | $pp \to H\,X$ | |
|---|---|---|---|
| ATLAS | $\mu_b = 0.98^{+0.22}_{-0.21}$ | $\mu_b = 1.01 \pm 0.20$ | [27] |
| CMS | $\mu_b = 1.01 \pm 0.22$ | $\mu_b = 1.04 \pm 0.20$ | [28] |

and for estimates we set

$$0.8 \leq \mu_b \leq 1.2 \tag{9}$$

Note, that the ratio (8) can be represented as follows:

$$\mu_b = \frac{\sigma^{exp}_{SM}(pp \to H\,X)\;\; B_{det}(H \to b\bar{b})_{SM}}{\sigma^{theor}_{SM}(pp \to H\,X)\;\; B_{det}(H \to b\bar{b})_{SM}}, \tag{10}$$

where $\mathcal{B}_{det}$ equals branching fractions of the Higgs decays into quark-antiquark pair ($B(H \to b\bar{b})_{SM}$) times the $B$-tagging efficiency ($\varepsilon_b$).

The anomalous $Hqq'$ FCNC interaction leads to modification of the ratio (10) in three moments:
(i) Higgs boson could produced thought $gg \to H$ and $q\bar{q}' \to H$ subprocess: $\sigma^{exp}_{SM}(pp \to H) \to \sigma(pp \to H)_{SM+FCNC}$;
(ii) the branching fraction should include the widths of $H \to q\bar{q}'$ decay channels;
(iii) the reconstructed $b\bar{b}$ final states should include the events with the Higgs decays into light quarks with the following light-quark misindentification as a $b$-jet.

However, the contributions to the Higgs production from anomalous $q\bar{q}' \to H$ subprocess with the $\lambda$ value from (6) is very small. Indeed, we use the MG5_aMC@NLO 2.5.2 [29] package (see section 3) for estimation of the Higgs anomalous production cross-sections at $\sqrt{s} = 13$ TeV:

$$\sigma_{SM} \approx 50\,\text{pb}$$
$$|\lambda_{qq'}| \leq 0.13 \Rightarrow \sigma(b\bar{s} + \bar{b}s)_{fcnc} = 3.0\,\text{pb},\;\; \sigma(b\bar{d} + \bar{b}d)_{fcnc} = 7.7\,\text{pb}$$

Therefore, we can ignore these FCNC contributions to the Higgs boson production. As a result, in order to get the constraints on anomalous constants $\lambda_{qq'}$ we consider the ratio:

$$r_b = \frac{\mathcal{B}_{det}(H \to b\bar{b})_{SM+FCNC}}{\mathcal{B}_{det}(H \to b\bar{b})_{SM}} \tag{11}$$

The value $\mathcal{B}_{det}$ equals branching fractions of the Higgs decays into quark-antiquark pair times the $B$-tagging and $B$ miss-tagging efficiencies (from ATLAS paper [27])

$$\varepsilon_b = 70\%,\;\; \varepsilon_c = 12\%,\;\; \varepsilon_q = 0.3\%,\;\; q = d, u, s \tag{12}$$

So, for SM and SM+FCNC scenarios we have:

$$\mathcal{B}_{det}(H \to b\bar{b})_{SM} = \mathcal{B}_{sm}(H \to b\bar{b})\varepsilon_b^2$$
$$\mathcal{B}_{det}(H \to b\bar{b})_{SM+FCNC} = B_{fcnc}(H \to b\bar{b})\varepsilon_b^2 + B_{fcnc}(H \to q_1\bar{q}_2)\varepsilon_{q_1}\varepsilon_{q_2}$$

Then, from the $\tilde{\mu}_b$ limits from (9) we get the constraints on the anomalous couplings $\lambda_{qq'}$ as well as on the branching ratios (see Table 3).

Certainly, these constraints are much worse than indirect constraints, given in the Table 2. Moreover, these estimates are very rough ones. However, more correct analysis (with Higgs decay into $b\bar{b}$ final state) is required the detail simulation of the events with signal and background contributions. This is out of scope of our study.

Table 3
The upper limits on the anomalous couplings, the Higgs boson decay widths (in MeV) and branching fractions.

| $qq'$ | $\lambda$ | $\Gamma(q\bar{q}')$ MeV | $\mathcal{B}(q\bar{q}')$ |
|---|---|---|---|
| $bs$ | 0.006 | 0.54 | 10% |
| $bd$ | 0.0063 | 0.60 | 11% |

Table 4
The cross-sections of Higgs boson + 0, 1 jet productions mediated by FCNC couplings in proton-proton collisions for different center-of-mass energies.

| Subprocess | Cross section, pb | | | |
|---|---|---|---|---|
| | 13 TeV | 14 TeV | 27 TeV | 100 TeV |
| $ucH$ | $9.08 \times 10^4 \lambda^2_{ucH}$ | $9.85 \times 10^4 \lambda^2_{ucH}$ | $2.01 \times 10^5 \lambda^2_{ucH}$ | $7.3 \times 10^5 \lambda^2_{ucH}$ |
| $dsH$ | $8.25 \times 10^4 \lambda^2_{dsH}$ | $9.02 \times 10^4 \lambda^2_{dsH}$ | $1.91 \times 10^5 \lambda^2_{dsH}$ | $7.23 \times 10^5 \lambda^2_{dsH}$ |
| $dbH$ | $4.81 \times 10^4 \lambda^2_{dbH}$ | $5.32 \times 10^4 \lambda^2_{dbH}$ | $1.18 \times 10^5 \lambda^2_{dbH}$ | $4.77 \times 10^5 \lambda^2_{dbH}$ |
| $sbH$ | $2.32 \times 10^4 \lambda^2_{sbH}$ | $2.61 \times 10^4 \lambda^2_{sbH}$ | $6.67 \times 10^4 \lambda^2_{sbH}$ | $3.27 \times 10^5 \lambda^2_{sbH}$ |

## 3. Event generation

The estimation based on (11) does not take into account the differences in kinematics of the SM and FCNC Higgs boson production processes. In order to accurately incorporate detector effects and reconstruction efficiencies for the next sections we are performing Monte-Carlo (MC) simulation of related processes. We use the Lagrangian (1) for the signal simulation. The Lagrangian (1) is implemented in FeynRules [30] based on [31] and the model is interfaced with generators using the UFO module [32]. The events are generated using the MG5_aMC@NLO 2.5.2 [29] package, with subsequent showering and hadronization in PYTHIA 8.230 [33]. The NNPDF3.0 [34] PDF sets are used. The detector simulation has been performed with the fast simulation tool DELPHES 3.4.2 [35] using the corresponding detectors parameterization cards. No additional pileup interactions are added to the simulation. The cross-sections for Higgs boson productions associated with zero or one jet and mediated by FCNC couplings in proton-proton collisions for different center-of-mass energy are given in the Table 4. Note, these values are evaluated for Higgs production with 0 or 1 jet using the MLM matching scheme [36]. Therefore, they are greater than those used in previous section.

## 4. Constrain from Higgs boson measurement in the four-lepton final state at $\sqrt{s} = 13$ TeV

In this section, we obtain the upper limit on the $\mathcal{B}(H \to b\bar{s})$ and $\mathcal{B}(H \to b\bar{d})$ branching fractions using constraints on Higgs boson measurement in the four-lepton final state at $\sqrt{s} = 13$ TeV from CMS experiment at LHC [37].

In order to accurately incorporate the effects of the analyses efficiency different for the SM and FCNC Higgs boson production we reproduce the events selections from [38]. While the gluon fusion ($ggH$), vector boson fusion (VBF) and associated production ($WH$, $ZH$ and $t\bar{t}H$) Higgs boson SM production processes are taken into account in the original analysis, the following selections are optimized for the $H \to ZZ \to 4\ell$ ($\ell = e$ or $\mu$) decay channel measurement and the information from associated particles in $H$ production is not used.

Table 5
The comparison of selection efficiency for FCNC and SM Higgs boson productions for different $ZZ$ decay channels before the cut on invariant mass reconstructed Higgs boson $m_{4l} \in [118, 130]$ GeV and after the cut. The reference Geant4 results are taken from [37].

| Higgs production | $4e$ | $2e2\mu$ | $4\mu$ | Total | Total ($m_{4l}$ cut) |
|---|---|---|---|---|---|
| SM (Geant4) | 5.1% | 13.1% | 10.5% | 28.8% | 25.5% |
| SM (Delphes) | 4.9% | 13.1% | 9.3% | 27.2% | 25.6% |
| FCNC ($dbH$) | 3.6% | 9.5% | 6.5% | 19.5% | 17.8% |
| FCNC ($sbH$) | 4.9% | 12.8% | 9% | 26.7% | 24.5% |

The four-lepton candidates build $ZZ$ pairs. One $Z$ candidate is defined as pairs of two opposite charge and matching flavor leptons ($e^+e^-$, $\mu^+\mu^-$) that satisfy $12 < m_{ll} < 120$ GeV. Electrons are reconstructed within the geometrical acceptance defined by pseudorapidity $|\eta^e| < 2.5$ and for transverse momentum $p_T^e > 7$ GeV. Muons are reconstructed within the geometrical acceptance $|\eta^\mu| < 2.4$ and $p_T^\mu > 5$ GeV. All leptons within $ZZ$ pairs must be separated in angular space by at least $\Delta R(l_i, l_j) > 0.02$. Two of the four selected leptons should have $p_{T,i} > 20$ GeV and $p_{T,j} > 10$ GeV.

The $Z$ candidate with reconstructed mass $m_{ll}$ closest to the nominal $Z$ boson mass is denoted as $Z_1$, and the second one is denoted as $Z_2$. The $Z_1$ invariant mass must be larger than 40 GeV. In the $4\mu$ and $4e$ sub-channels the $ZZ$ event with reconstructed mass $m_{Z2} \geq 12$ GeV and $m_{Z1}$ closest to the nominal $Z$ boson mass. All four opposite-charge lepton pairs that can be built with the four leptons (irrespective of flavor) are required to satisfy $m_{l_i^+ l_j^-} > 4$ GeV. Finally, the four-lepton invariant mass should be of the Higgs boson in a $118 < m_{4l} < 130$ GeV.

The comparison of selection efficiencies for FCNC Higgs boson production processes are presented in Table 5. The simulation of the SM Higgs boson production with Delphes show good agreement with reference Geant4 results taken from [37]. The selection efficiency is different for different FCNC Higgs boson productions processes due to the presence of the valence $d$ quark in $bdH$ vertex (as compared to $bs \to H$ production).

Statistical analyses are performed based on the number of selected events (after the cut on $118 < m_{4l} < 130$ GeV) where the expected number of signal FCNC events is from our modeling and the observed and expected number of background events are taken from the CMS experimental results [37]. For the signal processes lepton energy resolution (20%), lepton energy scale (0.3%), lepton identification (9% on the overall event yield) and luminosity (2.6%) uncertainties are taken into account. The uncertainty from the renormalization and factorization scale is determined by varying these scales between 0.5 and 2 times their nominal value while keeping their ratio between 0.5 and 2 [39]. PDF uncertainty is determined by taking the root mean square of the variation when using different replicas of the default PDF set [40]. Contributions of the systematic uncertainties to selection efficiency of the FCNC Higgs boson production are summarized in the Table 6. The total uncertainties on the number of selected signal and background (extracted from [37]) events are incorporated into statistical model as nuisances neglecting the correlations.

Bayesian inference is used to derive the posterior probability based on the following likelihood function:

$$\mathcal{L} = \mathcal{G}\left(N_{obs} | N_{back} + (N_{SM} + N_{FCNC}) \cdot \frac{\mathcal{B}_{FCNC+SM}}{\mathcal{B}_{SM}}, \sqrt{N_{obs}}\right) \times$$

Table 6
Summary of contribution of the systematic uncertainties to the selection efficiency of the FCNC Higgs boson production.

| Process | $\mathcal{B}(H \to b\bar{s})$ | $\mathcal{B}(H \to b\bar{d})$ |
|---|---|---|
| Lepton energy resolution | $< \pm 0.2\%$ | $< \pm 0.2\%$ |
| Lepton energy scale | $< \pm 0.5\%$ | $< \pm 0.5\%$ |
| Lepton identification | $\pm 9\%$ | $\pm 9\%$ |
| Luminosity | $\pm 2.6\%$ | $\pm 2.6\%$ |
| QCD scale | $-19.6\% +18.1$ | $-17\% +15.2\%$ |
| PDF | $\pm 8\%$ | $\pm 3.4$ |
| Total | $-23.1\% +21.9\%$ | $-19.7\% +18.2\%$ |

Table 7
Cross section ratios $\sigma_{14\text{ TeV}}/\sigma_{13\text{ TeV}}$ for FCNC and background processes.

| Process | $\sigma_{14\text{ TeV}}/\sigma_{13\text{ TeV}}$ |
|---|---|
| $qq \to ZZ$ | 1.17 |
| $gg \to ZZ$ | 1.13 |
| "$Z + X$" | 1.11 |
| SM Higgs | 1.13 |
| FCNC Higgs ($dbH$) | 1.10 |
| FCNC Higgs ($sbH$) | 1.13 |

$$\times \mathcal{G}\left(N_{back} | N^{exp}_{back}, \sigma_{N^{exp}_{back}}\right) \times$$
$$\times \mathcal{G}\left(N_{FCNC} | N^{exp}_{FCNC}(\lambda), \sigma_{N^{exp}_{FCNC}(\lambda)}\right)$$

where the $\mathcal{G}$ - Gaussian function, $N^{exp}_{back}$, $N^{exp}_{SM}$, $N^{exp}_{FCNC}$ - the expected from the MC simulation number of background, SM and FCNC Higgs boson production events respectively, $\sigma_{N^{exp}}$ - its uncertainty, $\mathcal{B}_{FCNC+SM}$ - branching of $H \to 4\ell$ ($\ell = e, \mu$) in the presence of FCNC.

The results of the statistical analysis are given in Table 8.

## 5. Sensitivity at HL-LHC

The reconstruction efficiency estimated in section 4 can be used to project the FCNC searches into HL-LHC conditions, defined by total integrated luminosity of 3 ab$^{-1}$ and collision energy of 14 TeV, respectively. For the rescaling the cross sections of SM Higgs boson productions are taken from [41]. The rescaling factors for cross sections of $qq \to ZZ$ and $gg \to ZZ$ background processes are taken from [42]. The rescaling factors for cross sections of "$Z + X$" background processes is estimated using the corresponding cross sections from MG5_aMC@NLO 2.5.2 [29] simulation of dominated $Z + jets$ process. The cross section ratio for the different processes are summarized in Table 7. Statistical analyses from section 4 is reproduced for the new conditions. The dominated systematic uncertainties on the simulation originating from theoretical sources are scaled by 50% following the treatment of systematic uncertainties in [41]. In this considered scenario the theoretical uncertainties are expected to improve over time due to developments in the calculations, techniques and orders considered. The results of the projection are summarized Table 8.

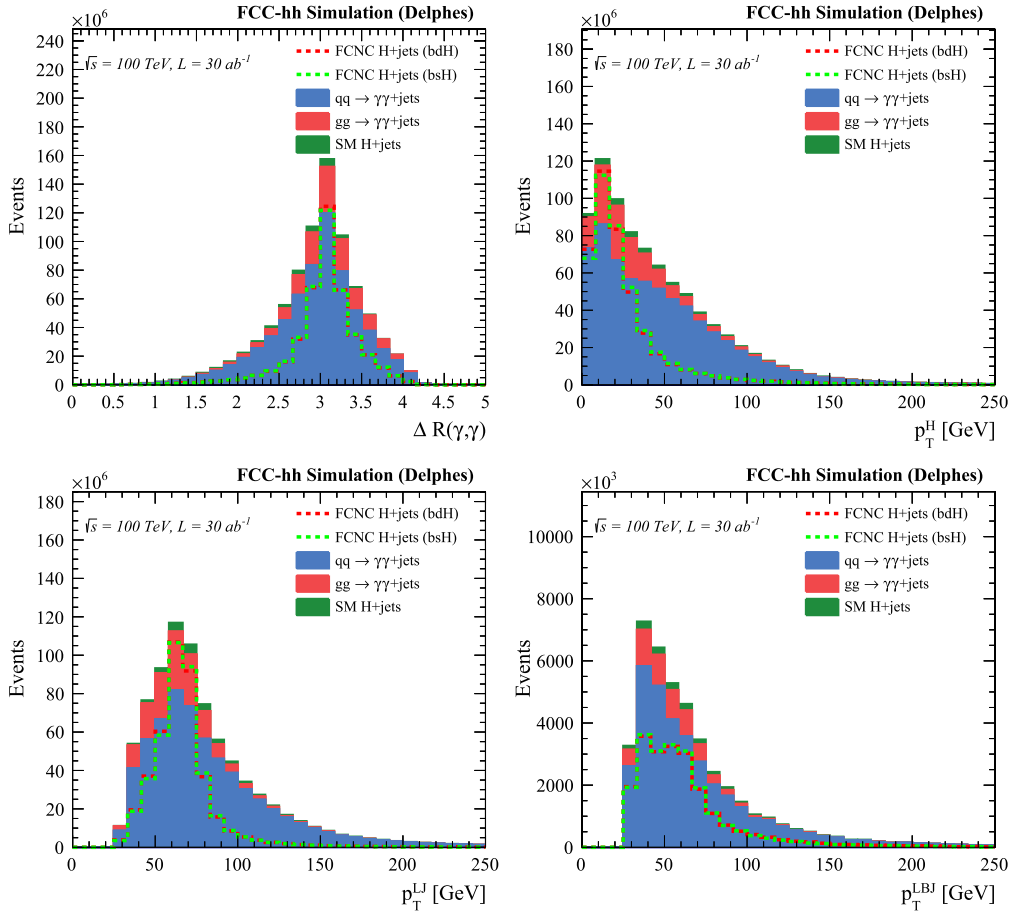


Fig. 2. Distributions of the kinematic variables obtained after basic selections: $\Delta R$ between two selected photons with the highest $p_T$ (top-left), $p_T$ of the Higgs boson candidate (top-right), $p_T$ of the leading jet (bottom-left), $p_T$ of the leading b-tagged jet (bottom-right). The signal processes have arbitrary normalization for the illustration purpose.

## 6. Sensitivity at FCC-hh

In this section the sensitivity to single Higgs boson production through FCNC in $bdH$ and $bsH$ subprocesses is explored for the FCC-hh experimental conditions following the [43] SM study. The $H \to \gamma\gamma$ decay channel is used in this analysis.

The background from QCD di-photon productions are considered in the analysis including the huge tree level $qq \to \gamma\gamma$ component, generated up to two merged extra-jets, and a smaller loop-induced component, $gg \to \gamma\gamma$, generated up to one additional merged jet. A conservative K-factor of 2 is applied to both QCD contributions. In addition, the four main SM single Higgs production modes are incorporated as backgrounds: gluon fusion production (ggF), vector boson fusion (VBF), top pair associated production (ttH) and Higgs-strahlung (VH).

The signal and background process generation and detector simulation are described in section 3.

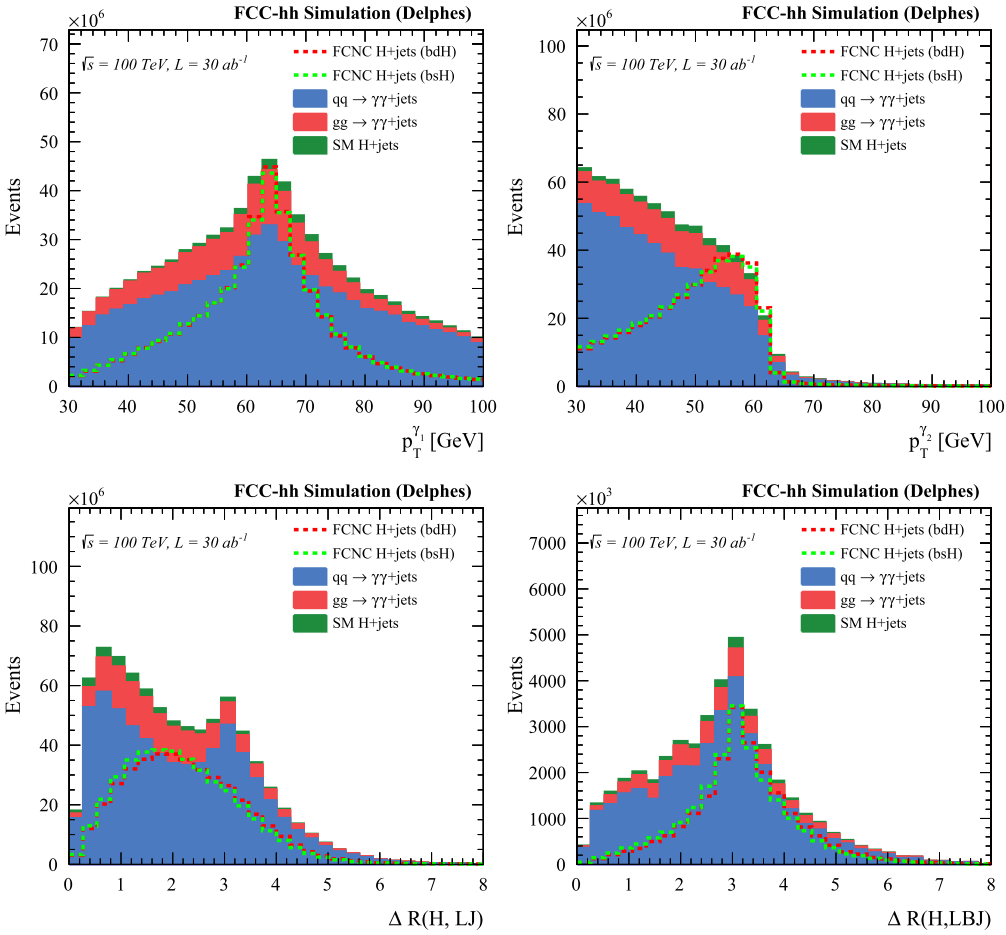


Fig. 3. Distributions of the kinematic variables obtained after basic selections: leading photons $p_T^{\gamma 1}$ (top-left), second photons $p_T^{\gamma 2}$ (top-right), $\Delta R$ between Higgs boson candidate and leading jet (bottom-left), $\Delta R$ between Higgs boson candidate and leading b-tagged jet (bottom-right). The signal processes have arbitrary normalization for the illustration purpose.

The photons with $p_T > 25$ GeV, $|\eta| < 4$ and relative isolation $< 0.15$ are used in the following analyses. Jets are reconstructed using anti$-kT$ algorithm with distance parameter $R = 0.4$ and required to have $p_T > 30$ GeV, $|\eta| < 3$. The events are selected using the following baseline criteria:

1. at least 2 selected photons and at least one of them with $p_T > 30$ GeV;
2. mass of the Higgs boson candidate reconstructed from the two photons with the highest $p_T$ should be $|m_H - 125| < 5$ GeV.

Distributions of the kinematic variables obtained after baseline selections are presented at Fig. 2, Fig. 3 and Fig. 4.

A Boosted Decision Tree (BDT) constructed in the TMVA framework [44] is used to separate the signal signature from the background contributions. For BDT training 10% of events are

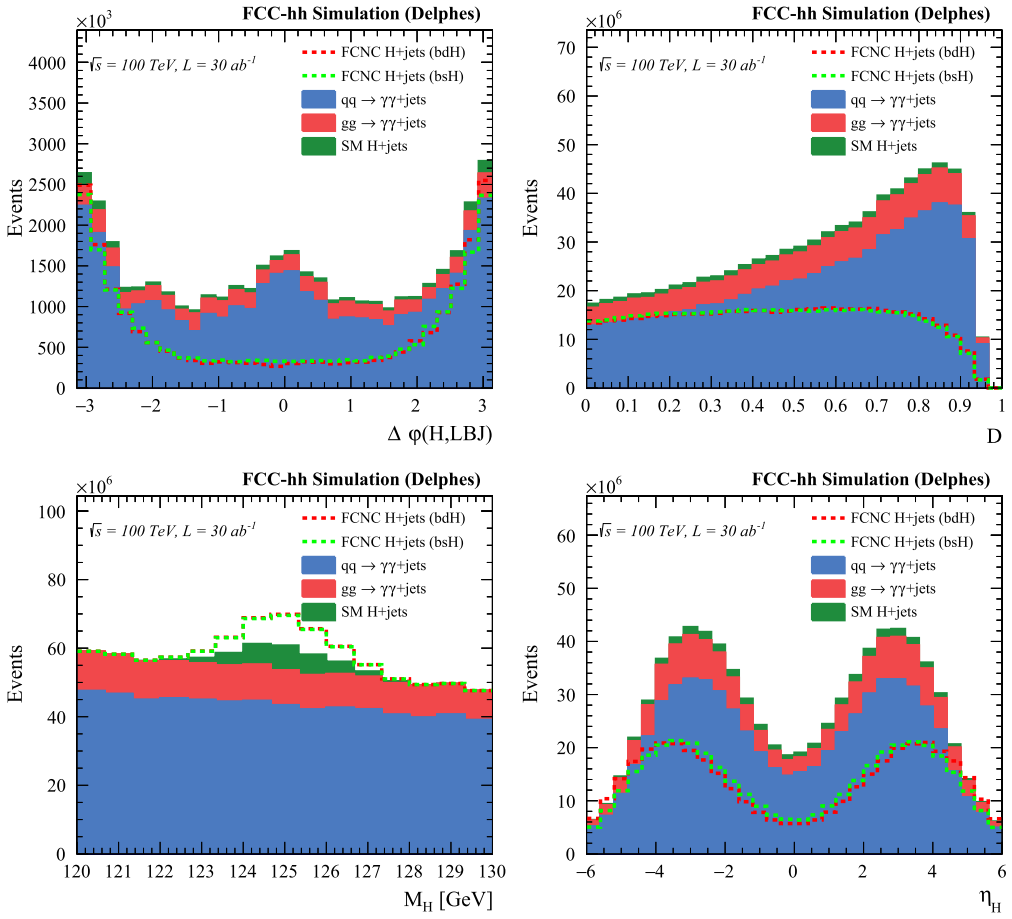


Fig. 4. Distributions of the kinematic variables obtained after basic selections: $\Delta\varphi$ between reconstructed Higgs boson candidate and leading b-tagged jet (top-left), disbalance in energy of photons from Higgs decay (top-right, see text for the description) and mass of the reconstructed Higgs boson candidate (bottom-left), $\eta$ of the reconstructed Higgs boson candidate (bottom-right). The signal processes have arbitrary normalization for the illustration purpose.

selected and the remainder are used in the statistical analysis with the CombinedLimit package. The following input variables are used for training:

1. Higgs boson candidate $M_H$, $p_T^H$ and $\eta_H$;
2. leading jet (LJ) $p_T^{LJ}$ and $\eta_{LJ}$;
3. leading b-tagged jet (LBJ) $p_T^{LBJ}$ and $\eta_{LBJ}$;
4. leading photons $p_T^{\gamma_1}$, $\eta^{\gamma_1}$ and second photons $p_T^{\gamma_2}$, $\eta^{\gamma_2}$;
5. Number of jets $N_{jets}$ and number of b-tagged jets $N_{b-jets}$;
6. $\Delta R(\gamma,\gamma)$ between leading and second photon;
7. $\Delta R(H, LBJ)$ between Higgs boson candidate and leading jet;
8. $\Delta R(H, LJ)$ between Higgs boson candidate and leading b-tagged jet.
9. disbalance in energy of photons from Higgs decay, defined as $D = \frac{|E_{\gamma_1} - E_{\gamma_2}|}{\max E_{\gamma_1}, E_{\gamma_2}}$

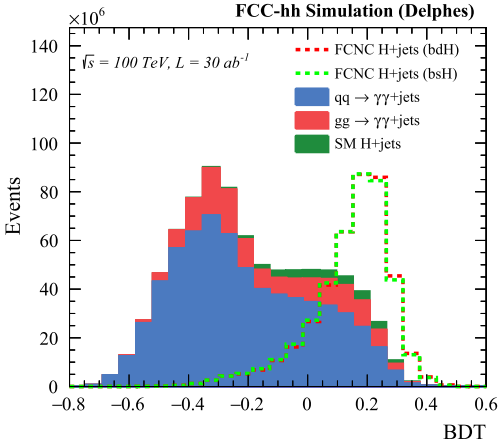


Fig. 5. The distribution of the BDT discriminant.

Table 8
The 95% C.L. expected exclusion limits at LHC(13 TeV), HL-LHC (14 TeV) and FCC-hh (100 TeV) on the branching fractions of Higgs FCNC decays and flavor-violating couplings in comparison with present experimental limits.

| Experiment | $\mathcal{B}(H \to b\bar{s})$ | $\mathcal{B}(H \to b\bar{d})$ |
|---|---|---|
| Meson oscillations [10] | $7 \times 10^{-3}$ | $8 \times 10^{-5}$ |
| CMS LHC $H \to ZZ \to 4\ell$ (137.1 fb $^{-1}$, 13 TeV) | $7.6 \times 10^{-2}$ | $8.0 \times 10^{-2}$ |
| HL-LHC $H \to ZZ \to 4\ell$ (3 ab$^{-1}$, 14 TeV) | $4.7 \times 10^{-2}$ | $4.9 \times 10^{-2}$ |
| FCC-hh $H \to \gamma\gamma$ (30 ab$^{-1}$, 100 TeV) | $1.5 \times 10^{-2}$ | $1.1 \times 10^{-2}$ |
| Experiment | $\lambda_{sbH}$ | $\lambda_{dbH}$ |
| Meson oscillations [10] | $1.9 \times 10^{-3}$ | $2.1 \times 10^{-4}$ |
| CMS LHC $H \to ZZ \to 4\ell$ (137.1 fb$^{-1}$, 13 TeV) | $6.9 \times 10^{-3}$ | $7.0 \times 10^{-3}$ |
| HL-LHC $H \to ZZ \to 4\ell$ (3 ab$^{-1}$, 14 TeV) | $3.6 \times 10^{-3}$ | $3.7 \times 10^{-3}$ |
| FCC-hh $H \to \gamma\gamma$ (30 ab$^{-1}$, 100 TeV) | $2.0 \times 10^{-3}$ | $1.8 \times 10^{-3}$ |

The distributions of the BDT discriminants (see Fig. 5) for backgrounds and signals are passed to the statistical analysis in order to construct binned likelihood function. The asymptotic frequentist formulae for profile likelihood ratio test statistic [45] is used to obtain an expected upper limit on signal cross section based on an Asimov data set of background-only model. For each background a 20% normalization uncertainty is assumed and incorporated in statistical model as nuisance parameter. The results of the analysis are given in Table 8. Fig. 6 shows the expected limits on the FCNC $H \to b\bar{s}$ and $H \to b\bar{d}$ branching fractions and FCNC couplings as a function of integrated luminosity.

## 7. Conclusions

In this work, we demonstrate that the contribution of flavor violation interaction to the production of the Higgs boson in high energy proton-proton collisions can be used for the direct search. The realistic detector simulation and accurately reproducing analysis selections of the CMS Higgs boson measurement in the four-lepton final state at $\sqrt{s} = 13$ TeV allow to set upper limits on the branching fractions of $H \to b\bar{s}$ and $H \to b\bar{d}$ and project the searches into HL-LHC

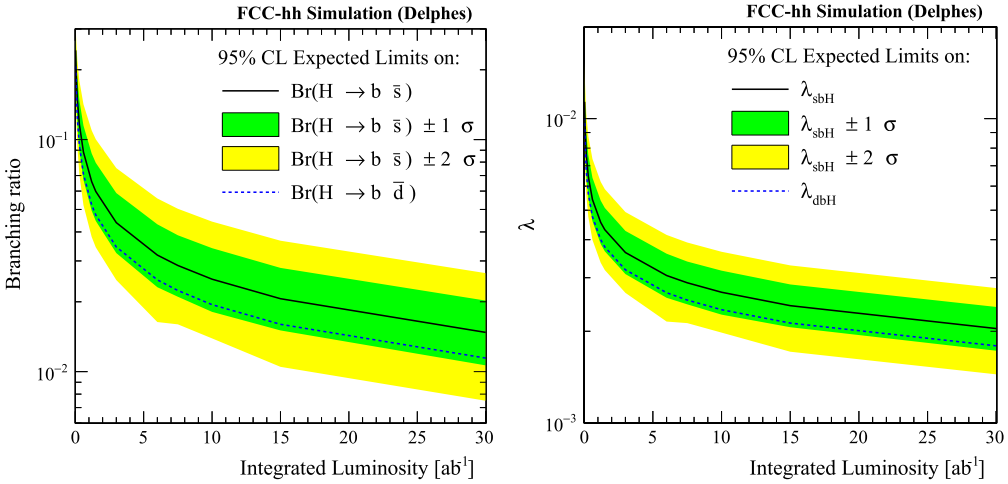


Fig. 6. The expected exclusion limits at 95% C.L. on the FCNC $H \to b\bar{s}$ and $H \to b\bar{d}$ branching fractions (left) and FCNC couplings (right) as a function of integrated luminosity, where $B(H \to qq') = \Gamma(H \to qq')/\Gamma_{tot}(H)$, with $\Gamma(H \to qq') = 6|\lambda_{qq'}|^2 M_H/(16\pi)$, see eq. (3).

conditions. We also examine the sensitivity at FCC-hh based on Higgs boson production with $H \to \gamma\gamma$ decay channel. Expected upper limits of the order of $10^{-2}$ at 95% CL for $\mathcal{B}(H \to b\bar{s})$ and $\mathcal{B}(H \to b\bar{d})$ are competitive with the indirect limits from meson oscillations experiments. The outcome of our study is summarized in Table 8. Further improvements are possible through the combination of results of different Higgs boson decay and interaction searches such as pair Higgs boson production.

## Acknowledgements

We are grateful to H. Gray, F. Moortgat and M. Selvaggi for permission to use the MC samples with background processes used in FCC-hh sensitivity study. We also would like to thank V.F. Kachanov and A.M. Zaitsev for useful discussions.

## References

[1] G. Aad, et al., Observation of a new particle in the search for the Standard Model Higgs boson with the ATLAS detector at the LHC, Phys. Lett. B 716 (2012) 1–29, https://doi.org/10.1016/j.physletb.2012.08.020, arXiv:1207.7214.

[2] S. Chatrchyan, et al., Observation of a new boson at a mass of 125 GeV with the CMS experiment at the LHC, Phys. Lett. B 716 (2012) 30–61, https://doi.org/10.1016/j.physletb.2012.08.021, arXiv:1207.7235.

[3] S.L. Glashow, J. Iliopoulos, L. Maiani, Weak interactions with lepton-hadron symmetry, Phys. Rev. D 2 (1970) 1285–1292, https://doi.org/10.1103/PhysRevD.2.1285.

[4] G. Aad, et al., Search for flavour-changing neutral current top quark decays $t \to Hq$ in $pp$ collisions at $\sqrt{s} = 8$ TeV with the ATLAS detector, J. High Energy Phys. 12 (2015) 061, https://doi.org/10.1007/JHEP12(2015)061, arXiv:1509.06047.

[5] M. Aaboud, et al., Search for top quark decays $t \to qH$, with $H \to \gamma\gamma$, in $\sqrt{s} = 13$ TeV $pp$ collisions using the ATLAS detector, J. High Energy Phys. 10 (2017) 129, https://doi.org/10.1007/JHEP10(2017)129, arXiv:1707.01404.

[6] M. Aaboud, et al., Search for flavor-changing neutral currents in top quark decays $t \to Hc$ and $t \to Hu$ in multi-lepton final states in proton–proton collisions at $\sqrt{s} = 13$ TeV with the ATLAS detector, arXiv:1805.03483.

[7] M. Aaboud, et al., Search for top-quark decays $t \to Hq$ with 36 fb$^{-1}$ of $pp$ collision data at $\sqrt{s} = 13$ TeV with the ATLAS detector, J. High Energy Phys. 05 (2019) 123, https://doi.org/10.1007/JHEP05(2019)123, arXiv:1812.11568.

[8] V. Khachatryan, et al., Search for top quark decays via Higgs-boson-mediated flavor-changing neutral currents in pp collisions at $\sqrt{s} = 8$ TeV, J. High Energy Phys. 02 (2017) 079, https://doi.org/10.1007/JHEP02(2017)079, arXiv:1610.04857.

[9] A.M. Sirunyan, et al., Search for the flavor-changing neutral current interactions of the top quark and the Higgs boson which decays into a pair of b quarks at $\sqrt{s} = 13$ TeV, arXiv:1712.02399, https://doi.org/10.1007/JHEP06(2018)102.

[10] R. Harnik, J. Kopp, J. Zupan, Flavor violating Higgs decays, J. High Energy Phys. 03 (2013) 026, https://doi.org/10.1007/JHEP03(2013)026, arXiv:1209.1397.

[11] A. Crivellin, J. Heeck, D. Müller, Large $h \to bs$ in generic two-Higgs-doublet models, Phys. Rev. D 97 (3) (2018) 035008, https://doi.org/10.1103/PhysRevD.97.035008, arXiv:1710.04663.

[12] W. Altmannshofer, B. Maddock, D. Tuckler, Rare top decays as probes of flavorful Higgs bosons, arXiv:1904.10956.

[13] P. Mandrik, Top FCNC searches at HL-LHC with the CMS experiment, EPJ Web Conf. 191 (2018) 02009, https://doi.org/10.1051/epjconf/201819102009, arXiv:1808.09915.

[14] D. Barducci, A.J. Helmboldt, Quark flavour-violating Higgs decays at the ILC, J. High Energy Phys. 12 (2017) 105, https://doi.org/10.1007/JHEP12(2017)105, arXiv:1710.06657.

[15] P. Mandrik, Prospect for top quark FCNC searches at the FCC-hh, in: 4th International Conference on Particle Physics and Astrophysics, ICPPA 2018, Moscow, Russia, October 22–26, 2018, 2018, arXiv:1812.00902.

[16] M.A. Arroyo-Ureña, R. Gaitán-Lozano, J.H. Montes de Oca Y., E.A. Herrera-Chacón, T.A. Valencia-Pérez, Search for the $t \to ch$ decay at hadron colliders, arXiv:1903.02718.

[17] G. Apollinari, I. Béjar Alonso, O. Brüning, M. Lamont, L. Rossi, High-Luminosity Large Hadron Collider (HL-LHC): Preliminary Design Report, CERN Yellow Reports: Monographs, CERN, Geneva, 2015, https://cds.cern.ch/record/2116337.

[18] A. Abada, et al., FCC Collaboration, FCC-hh: The Hadron Collider: Future Circular Collider Conceptual Design Report Volume 3, Eur. Phys. J. Spec. Top. 228 (4) (2019) 755, https://doi.org/10.1140/epjst/e2019-900087-0.

[19] A. Abada, et al., FCC Collaboration, FCC Physics Opportunities: Future Circular Collider Conceptual Design Report Volume 1, Eur. Phys. J. C 79 (6) (2019) 474, https://doi.org/10.1140/epjc/s10052-019-6904-3.

[20] K. Agashe, et al., Working group report: top quark, in: Proceedings, 2013 Community Summer Study on the Future of U.S. Particle Physics: Snowmass on the Mississippi, CSS2013, Minneapolis, MN, USA, July 29-August 6, 2013, 2013, arXiv:1311.2028, https://inspirehep.net/record/1263763/files/1311.2028.pdf.

[21] S. Weinberg, Phenomenological Lagrangians, Physica A 96 (1–2) (1979) 327–340, https://doi.org/10.1016/0378-4371(79)90223-1.

[22] W. Buchmuller, D. Wyler, Effective Lagrangian analysis of new interactions and flavor conservation, Nucl. Phys. B 268 (1986) 621–653, https://doi.org/10.1016/0550-3213(86)90262-2.

[23] C. Arzt, M.B. Einhorn, J. Wudka, Patterns of deviation from the standard model, Nucl. Phys. B 433 (1995) 41–66, https://doi.org/10.1016/0550-3213(94)00336-D, arXiv:hep-ph/9405214.

[24] J.A. Aguilar-Saavedra, Top flavor-changing neutral interactions: theoretical expectations and experimental detection, Acta Phys. Pol. B 35 (2004) 2695–2710, arXiv:hep-ph/0409342.

[25] J.A. Aguilar-Saavedra, A minimal set of top-Higgs anomalous couplings, Nucl. Phys. B 821 (2009) 215–227, https://doi.org/10.1016/j.nuclphysb.2009.06.022, arXiv:0904.2387.

[26] A.M. Sirunyan, et al., Measurements of the Higgs boson width and anomalous $HVV$ couplings from on-shell and off-shell production in the four-lepton final state, Phys. Rev. D 99 (11) (2019) 112003, https://doi.org/10.1103/PhysRevD.99.112003, arXiv:1901.00174.

[27] M. Aaboud, et al., Observation of $H \to b\bar{b}$ decays and $VH$ production with the ATLAS detector, Phys. Lett. B 786 (2018) 59–86, https://doi.org/10.1016/j.physletb.2018.09.013, arXiv:1808.08238.

[28] A.M. Sirunyan, et al., Observation of Higgs boson decay to bottom quarks, Phys. Rev. Lett. 121 (12) (2018) 121801, https://doi.org/10.1103/PhysRevLett.121.121801, arXiv:1808.08242.

[29] J. Alwall, R. Frederix, S. Frixione, V. Hirschi, F. Maltoni, O. Mattelaer, H.S. Shao, T. Stelzer, P. Torrielli, M. Zaro, The automated computation of tree-level and next-to-leading order differential cross sections, and their matching to parton shower simulations, J. High Energy Phys. 07 (2014) 079, https://doi.org/10.1007/JHEP07(2014)079, arXiv:1405.0301.

[30] A. Alloul, N.D. Christensen, C. Degrande, C. Duhr, B. Fuks, FeynRules 2.0 - a complete toolbox for tree-level phenomenology, Comput. Phys. Commun. 185 (2014) 2250–2300, https://doi.org/10.1016/j.cpc.2014.04.012, arXiv:1310.1921.

[31] A. Amorim, J. Santiago, N. Castro, R. Santos, http://feynrules.irmp.ucl.ac.be/wiki/GeneralFCNTop.
[32] C. Degrande, C. Duhr, B. Fuks, D. Grellscheid, O. Mattelaer, T. Reiter, UFO - The Universal FeynRules Output, Comput. Phys. Commun. 183 (2012) 1201–1214, https://doi.org/10.1016/j.cpc.2012.01.022, arXiv:1108.2040.
[33] T. Sjöstrand, S. Ask, J.R. Christiansen, R. Corke, N. Desai, P. Ilten, S. Mrenna, S. Prestel, C.O. Rasmussen, P.Z. Skands, An introduction to PYTHIA 8.2, Comput. Phys. Commun. 191 (2015) 159–177, https://doi.org/10.1016/j.cpc.2015.01.024, arXiv:1410.3012.
[34] R.D. Ball, et al., Parton distributions for the LHC Run II, J. High Energy Phys. 04 (2015) 040, https://doi.org/10.1007/JHEP04(2015)040, arXiv:1410.8849.
[35] J. de Favereau, C. Delaere, P. Demin, A. Giammanco, V. Lemaître, A. Mertens, M. Selvaggi, Delphes 3: a modular framework for fast simulation of a generic collider experiment, J. High Energy Phys. 2014 (2) (2014) 57, https://doi.org/10.1007/JHEP02(2014)057.
[36] J. Alwall, et al., Comparative study of various algorithms for the merging of parton showers and matrix elements in hadronic collisions, Eur. Phys. J. C 53 (2008) 473–500, https://doi.org/10.1140/epjc/s10052-007-0490-5, arXiv:0706.2569.
[37] Measurements of properties of the Higgs boson in the four-lepton final state in proton-proton collisions at $\sqrt{s} =$ 13 TeV, Tech. Rep. CMS-PAS-HIG-19-001, CERN, Geneva, 2019, https://cds.cern.ch/record/2668684.
[38] A.M. Sirunyan, et al., Measurements of properties of the Higgs boson decaying into the four-lepton final state in pp collisions at $\sqrt{s} = 13$ TeV, J. High Energy Phys. 11 (2017) 047, https://doi.org/10.1007/JHEP11(2017)047, arXiv:1706.09936.
[39] D. de Florian, et al., Handbook of LHC Higgs cross sections: 4. Deciphering the nature of the Higgs sector, arXiv:1610.07922, https://doi.org/10.23731/CYRM-2017-002.
[40] J. Butterworth, et al., PDF4LHC recommendations for LHC Run II, J. Phys. G 43 (2016) 023001, https://doi.org/10.1088/0954-3899/43/2/023001, arXiv:1510.03865.
[41] M. Cepeda, et al., Higgs physics at the HL-LHC and, HE-LHC, arXiv:1902.00134.
[42] Vector Boson Scattering prospective studies in the ZZ fully leptonic decay channel for the high-Luminosity and High-Energy LHC upgrades, Tech. Rep. CMS-PAS-FTR-18-014, CERN, Geneva, 2018, http://cds.cern.ch/record/2650915.
[43] L. Borgonovi, et al., Higgs measurements at FCC-hh, Tech. Rep. CERN-ACC-2018-0045, CERN, Geneva, Oct. 2018, https://cds.cern.ch/record/2642471.
[44] A. Hocker, et al., TMVA - Toolkit for Multivariate Data Analysis, arXiv:physics/0703039.
[45] G. Cowan, K. Cranmer, E. Gross, O. Vitells, Asymptotic formulae for likelihood-based tests of new physics, Eur. Phys. J. C 71 (2011) 1554, https://doi.org/10.1140/epjc/s10052-011-1554-0, arXiv:1007.1727;
G. Cowan, K. Cranmer, E. Gross, O. Vitells, Eur. Phys. J. C 73 (2013) 2501, https://doi.org/10.1140/epjc/s10052-013-2501-z (Erratum).